Desalination and Water Treatment
www.deswater.com

doi: 10.5004/dwt.2018.21938

108 (2018) 291–298
March

Separation of direct orange S from wastewater by the ceramic membranes with Ce/Sb-SnO_2

Yu-Jiang Guan[a,*], Yi-Lin Shang[b], Zi-Bo Wang[b], Sheng-Tao Jiang[a]

[a]*Department of Environmental Engineering, Taizhou University, Taizhou 318001, Zhejiang, China, Tel. +86-576-88660340; emails: gyujiang@126.com (Y.-J. Guan), jst80@126.com (S.-T. Jiang)*
[b]*College of Environmental Science and Engineering, Yangzhou University, Yangzhou 225127, Jiangsu, China, Tel. +86-514-87978626; emails: 766110016@qq.com (Y.-L. Shang), wangzb@yzu.edu.cn (Z.-B. Wang)*

Received 15 April 2017; Accepted 26 January 2018

ABSTRACT

This paper explores ceramic membrane with Ce/Sb-SnO_2 separating dye from wastewater and its application. First of all, a ceramic membrane was coated by 4A zeolite for reducing its pores. Subsequently, Ce/Sb-SnO_2 sol was applied to the ceramic to prepare Ce/Sb-SnO_2 membranes. Scanning electron microscopic images revealed that SnO_2 nanoparticles were loaded on a ceramic matrix to form the composite membranes. From energy-dispersive X-ray and X-ray diffraction analysis, Ce, Sb and SnO_2 were confirmed to exist in the prepared samples. Ce/Sb-SnO_2 membrane was employed to separate direct orange S from wastewater and a retention rate of 99% for dye was obtained at transmembrane pressure of 0.6 MPa, dye concentration of 20 mg L^{-1} and voltage 1.4 V.

Keywords: Membrane separation; Electrocatalysis; Ce/Sb-doped SnO_2; Membrane fouling

1. Introduction

Dyeing effluents from textile industry are high contaminated wastewater containing a high content of dyes, inorganic salt, toxicants and hard-degraded organics, which give rise to harmful effects to the environment [1,2]. Many technologies, such as physical adsorption, biodegradation and chemical oxidation [3,4], have been developed to treat dye wastewater. However, dyeing wastewater treatment by chemical methods, high sludge and secondary reaction are produced. Hence, chemical methods have some limitations in dyeing effluents treatment and are not suited to degrade all dyes [5].

We imagine that dyes were separated from dyeing effluents by membranes and recycled as useful resource to avoid polluting environment. Nanofiltration process with the low energy consumption is suitable for separation and recycling of dyestuff from wastewater. The key problem of membrane separation is to control membrane fouling. While dyes are separated from wastewater by membranes, some of dyes are adsorbed on membrane surfaces to plug pores, which results in permeate flux decline [6,7]. Brillas and Martínez-Huitleb [8] reported that organic dyes in industrial effluents could be removed by electrochemical methods. Organic dyes are decomposed by electrocatalysts in the presence of power supply, which is mainly ascribed to produce reactive species such as hydroxyl radicals (•OH). Physisorbed hydroxyl radicals on electrodes have high reactivity towards most organic substrates, and they are readily reacting with organic dyes on electrode surfaces, and then the organic dyes are degraded to form CO_2 and H_2O. Based on this reason, electrocatalysts are introduced on the membrane surfaces for removing pollutants on the membrane surfaces [9] to avoid membrane pores to be plugged. Therefore, the integrated coupling of electrocatalysis and membrane separation, the membrane separation efficiency can be improved, which enhances the working stability of the membrane and prolongs its service life.

In this work, the ceramic membrane loaded with electrocatalysts was used to separate dyes from wastewater.

* Corresponding author.

It is well known that ceramic membrane has properties of antioxidation, high temperature resistance and acid-proof alkali. Hence, ceramic membrane may be used as matrix materials, on which metals and metallic oxide catalysts are loaded in order to enhance membrane's conductivity [10,11]. Using the membranes with electrocatalysts to separate dyes from wastewater, electrocatalytic oxidation can inhibit membrane fouling. Dong et al. [12–14] reported that electric field can reduce membrane fouling and improve membrane separation efficiency, and the pure water flux and bovine serum albumin rejection could be increased by hybrid polyvinylidene fluoride/Al_2O_3 membranes. Moreover, it was reported that tin dioxide as electrocatalyst had an excellent catalytic activity in wastewater treatment [15,16]. SnO_2 doped with Sb, its electrocatalytic property was further enhanced [17]. Since atomic weight of Sn and Sb is 118.71 and 121.75, respectively, atomic radius of Sb is approximate to that of Sn. Therefore, Sb could be chosen as a dopant. In addition, an antierosion ability of a single dopant is not strong enough and the choices of dopants are developed from a single to complex directions. It was reported that SnO_2 doped with Ce, its sintering properties was improved, which enhanced the densification of the prepared samples [18]. Based on the respective properties of Sb and Ce, SnO_2 modified with Ce/Sb was anchored on a ceramic, and both separation and electrocatalysis could be carried out simultaneously on membranes with Ce/Sb-SnO_2. By the analysis above, we could speculate that the ceramic membranes with Ce/Sb-SnO_2 were expected to possess an excellent ability to separate dyes and to reduce the membrane fouling at the same time.

Direct orange S dye is used to stain cellulose fibre such as linen, viscose rayon, cotton, etc. To date, there are no reports on the ceramic membranes with Ce/Sb-SnO_2 separating dyes from wastewater. In this work, direct orange S was chosen as target pollutant to evaluate the separation properties of the membranes with Ce/Sb-SnO_2. We reported the preparation of the Ce/Sb-SnO_2 membrane and its application in separation of dye from wastewater.

2. Experimental details

2.1. Materials and apparatus

Main chemicals and reagents used include the following: sodium hydroxide, tin dioxide, absolute ethanol, concentrated hydrochloric acid, sodium silicate, cerium nitrate, antimony trichloride, sodium meta-aluminate, and all reagents used were purchased commercially and were of analytical grade.

Main methods used in this study include the following: X-ray diffractometer (XRD; Bruker AXS, Germany), scanning electron microscope (SEM; S-4800, Hitachi, Japan), acquisition unit (Rui Bohua Technology Co., Ltd., Beijing, China), electrochemical analyzer (PAR 273 A, Princeton Research Company of Chemical Application, America), energy-dispersive X-ray (EDX; 250, Hitachi, Japan), spectrophotometer (Cary50, US Varian Technology Co., Ltd., China) and total organic carbon analyzer (TOC-V CPH; Shimadu, Japan) were employed to characterize the prepared samples and analyze experimental results.

2.2. Preparation of Ce/Sb-SnO_2 ceramic membranes

The sodium silicate solution was prepared by adding 0.32 g of sodium hydroxide and 18 mL of deionized water to 5.68 g of sodium silicate with magnetic stirrer at 298 K. The sodium aluminate solution was prepared by adding 15 mL of deionized water to 1.64 g of sodium meta-aluminate with magnetic stirrer at 298 K. Subsequently, the sodium aluminate solution was slowly dripped into the sodium silicate solution, which was aged for 2 d and called as the solution (A).

Origin ceramic membranes were made from Al_2O_3–SiO_2–ZrO_2 and a disc membrane with a diameter of 51 mm, thickness of 6 mm and a pore size of 50–100 nm, and were purchased from Fucide New Material Co., Ltd. (Anhui, China). A side of the membrane surfaces was steeped into the solution (A), and sealed in reaction kettle and crystallized for 5 h at 393 K. As a result, a side of the membrane surfaces was successfully coated by the 4A zeolite for reducing its pores.

A SnO_2 sol was prepared by adding 25 mL of absolute ethanol and 2 mL of hydrochloric acid to 14.73 g of tin dioxide with magnetic stirrer at 298 K. Antimony trichloride (1.84 g) was put into the SnO_2 sol in order to prepare the Sb-SnO_2 sol. Cerium nitrate solution was prepared by adding 10 mL of absolute ethanol and 2 mL of deionized water to 0.35 g of cerium nitrate with magnetic stirrer at 298 K.

With a dripping speed of 1 mL min^{-1}, the cerium nitrate solution was slowly dripped into Sb-SnO_2 sol with magnetic stirrer at 313 K to form Ce/Sb-SnO_2 sol. In the Ce/Sb-SnO_2 sol, the mole ratio of Ce, Sb and SnO_2 was nearly 1:10:100, and the results were satisfactory in experimentation. A side of ceramic membranes coated with the 4A zeolite was steeped into Ce/Sb-SnO_2 sol for 30 min and kept for 1 h at 298 K, and calcined at 1,173 K for 2 h in N_2 atmosphere with a heating rate of 3 K min^{-1}, and cooled to room temperature. As a result, Ce/Sb-SnO_2 was successfully loaded on a side of the ceramic membranes, labelled as the ceramic membranes with Ce/Sb-SnO_2.

2.3. Experimental setup

Experimental apparatus used in this study is demonstrated in Fig. 1. A ceramic membrane reactor was made of a reaction chamber (12), ceramic membrane with Ce/Sb-SnO_2 (3) and a separation chamber (4). Artificial dye wastewater was used in this study and it was only a direct orange S dye solution. Dye solution (8) was carried to a reaction chamber (12) by diaphragm pump with a feed flow of 3.5 L min^{-1}. While the dye from solution in a reaction chamber was separated by membranes with Ce/Sb-SnO_2, pollutants absorbed on membrane surfaces were simultaneously decontaminated by catalytic oxidation. Both separation of dyes and electrocatalytic reaction were carried out on this membrane with Ce/Sb-SnO_2 in the presence of power supply. As a result, the permeated solution was in a separation chamber and the concentrated solution was in a reaction chamber. The velocities of cross-flow (CF) and transmembrane pressure in separation process were regulated by valve (10), and dye solution pH was adjusted by using HCl or NaOH solution.

The maximum absorption wavelength of direct orange S is 312 nm. Dye concentration in wastewater was determined by UV–vis spectroscopy at 312 nm.

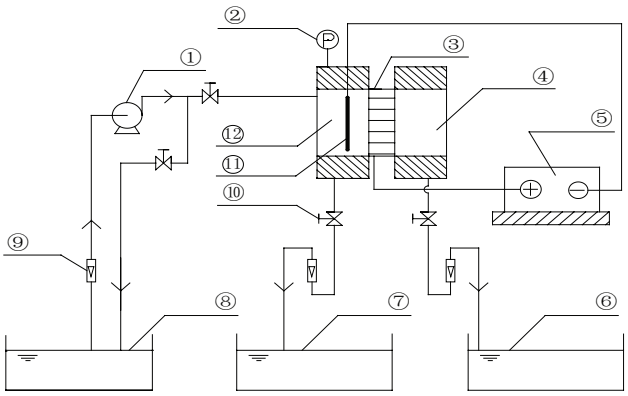

Fig. 1. Process of membrane separation with electrocatalysis. Notes: (1) diaphragm pump; (2) pressure gauge; (3) ceramic membrane; (4) separation chamber; (5) voltage-stabilized source; (6) permeated solution; (7) concentrated solution; (8) dye-containing aqueous solution; (9) flow meter; (10) adjustment valve; (11) cathode and (12) reaction chamber.

3. Results and discussion

3.1. Characterization of samples synthesized

SEM images of the ceramic membranes are shown in Fig. 2(a), and the surfaces had some larger pores and irregular defects. Fig. 2(b) shows that membrane surfaces were mainly filled by 4A zeolite, but the surfaces had still some defects. Ce/Sb-SnO_2 was loaded on the defective surfaces in order to prepare sample membranes. Fig. 2(c) shows that the samples were possessed of good microstructure morphology. With the molecular weight cut-off of polyethylene glycol (PEG) methods, according to calculation from the following equation [19]:

$$\text{Molecular radius (Å)} = 0.262 \times (\text{MW})^{1/2} - 0.3 \quad (1)$$

Hence, an average pore size of the Ce/Sb-SnO_2 and the Sb-SnO_2 membranes was calculated to be 1.95 and 2.86 nm, respectively. In Figs. 11(a) and (b), although the magnification of membrane surface morphology is only 500 times, the authors think that the differences of the two membrane surface morphologies can be clearly observed. In future studies, they will make the magnification of membrane surface morphologies over 500 times to observe the differences among morphologies.

Fig. 3 shows the EDX patterns of origin ceramic membrane and the prepared samples, and the samples containing elements Ce, Sb, Sn and O. Table 1 shows the composition of the origin ceramic. In Table 2, the mass percentages of tin and oxygen were 54.59% and 32.94%, respectively. The mass ratio of tin to oxygen was 1.66. The percentages of atoms for tin and oxygen were 28.41% and 60.91%, respectively. Therefore, the ratio of atoms for tin to oxygen was calculated to be 1.00:2.14 in the prepared samples. In theory, the ratio of atoms for tin to oxygen should be 1:2 in SnO_2. The experimental result (1:2.14) was nearly consistent with the theoretical value (1:2).

Fig. 4 shows the XRD patterns of the Sb-SnO_2 and Ce/Sb-SnO_2. According to the powder diffraction file (PDF) No. 01-0657 and PDF No. 01-0625, the characteristic peak at 26.56°, 33.75° and 51.64° can be indexed to crystal faces (110),

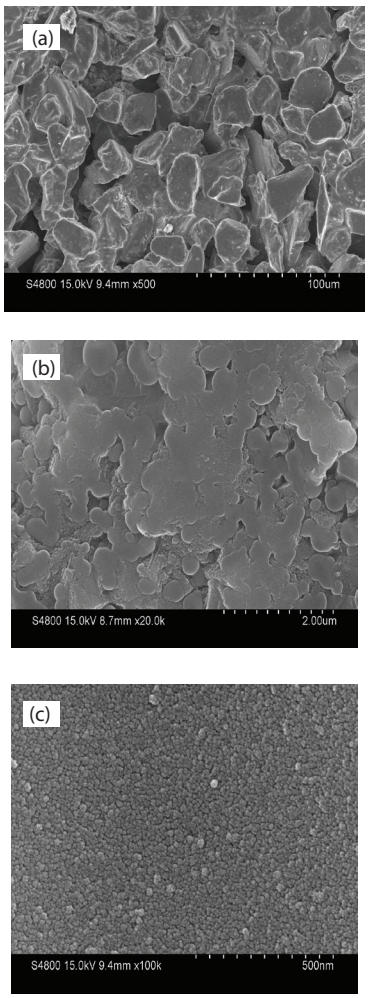

Fig. 2. SEM images of (a) ceramic membranes, (b) 4A zeolite/ceramic membrane and (c) Ce/Sb-SnO_2/4A zeolite/ceramic membrane.

(101) and (211) of tetragonal crystal shape of SnO_2, respectively. Therefore, SnO_2 was confirmed to exist in the samples synthesized. According to the PDF No. 33-0110 and 02-1385, the characteristic peaks at 37.77° and 65.18° are attributed to crystal faces (020) of monoclinic crystal shape and (711) of cubic crystal shape of Sb_2O_5, respectively. The small peaks at 65.39°, 70.73° and 78.56° can be indexed to crystal faces (501), (226) and (424) of hexagonal crystal shape of CeO_2 (PDF No. 44-1001), respectively. Since the prepared samples containing Ce and Sb were calcined at high temperature, the Ce and Sb oxide were confirmed to exist in the samples.

With Scherrer formula ($d = 0.89\lambda/\beta\cos\theta$), for the Ce/Sb-$SnO_2$, an average diameter of SnO_2 crystals was calculated to be 8.5 nm. For the Sb-SnO_2, an average diameter of SnO_2 was 9.7 nm. Since Ce was doped into Sb-SnO_2 sol, the crystallinity of Sb-SnO_2 sol was affected and the growth of SnO_2 crystal grains was inhibited. Because of Ce and Sb doped into SnO_2 sol, the Ce/Sb-SnO_2 was conjectured to possess a hybrid structure, which helps to increase dispersity of SnO_2 nanoparticles on membrane surface. Smaller SnO_2 crystals with a huge surface area can improve their stabilities and catalytic activities, and also provide more active sites

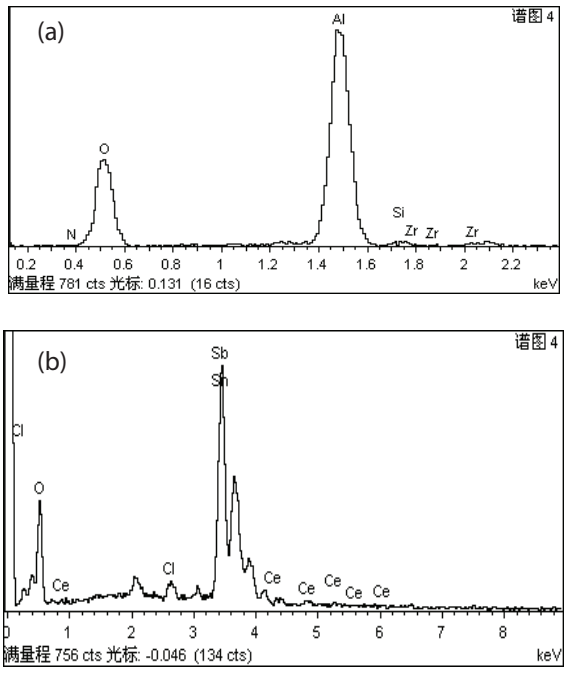

Fig. 3. EDX patterns of (a) ceramic and (b) membranes with Ce/Sb-SnO_2 membranes.

Table 1
Composition of origin ceramic membrane

Elements	Mass percentage (%)	Percentage of atoms (%)
N	8.38	11.48
O	49.80	59.76
Al	39.04	27.78
Si	0.83	0.57
Zr	1.95	0.41
Total	100.00	100.00

Table 2
Relative percentage of elements and atoms

Elements	Mass percentage (%)	Percentage of atoms (%)
O	32.94	60.91
Cl	1.21	0.29
Sn	54.59	28.41
Sb	8.81	9.37
Ce	2.46	0.66
Total	100.00	100.00

for electrocatalytic reaction. Hence, it is suggested that the Ce/Sb-SnO_2 membranes synthesized would present a better electrocatalytic activities in comparison with the Sb-SnO_2 ones.

3.2. Analysis of CV curves

Cyclic voltammetry (CV) curves for the Sb-SnO_2 and Ce/Sb-SnO_2 membrane in 0.1 M KCl solution containing

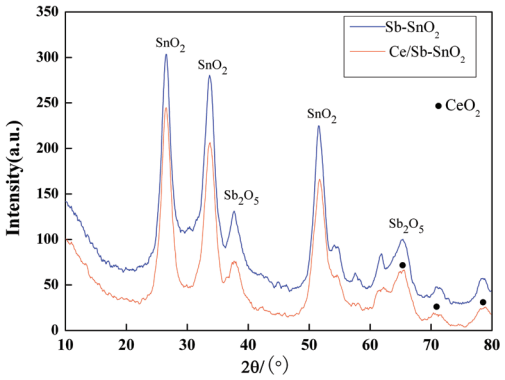

Fig. 4. XRD patterns of Sb-SnO_2 and Ce/Sb-SnO_2.

10 mM $K_3[Fe(CN)_6]$ are shown in Fig. 5. CV tests were carried out to evaluate electrochemical properties of the samples synthesized. As shown in Fig. 5, with a scan rate of 100 mV s^{-1}, the potential ranged from –1.0 to 1.0 V vs. the saturated calomel electrode.

Fig. 5(a) shows that the CV curves display a small oxidation current peak for $Fe(CN)_6^{3-/4-}$ redox and also showed quasi-irreversible processes. In Fig. 5(a), the oxidation current peak corresponding to $Fe(CN)_6^{3-/4-}$ redox transition is observed at about –0.436 V. In Fig. 5(b), a small weak oxidation current peak is observed at about –0.852 V. No deoxidization current peaks are obviously observed in Fig. 5. From the above results, this indicated that doping of Ce did not improve electrocatalytic oxidation activity of Ce/Sb-SnO_2, and only improved sintering properties of the sample membranes [18]. XRD and EDX analysis confirmed that the Ce/Sb-SnO_2 was loaded on a ceramic. Since the ceramic membranes with Ce/Sb-SnO_2 were found to be stable and reusable in experiments, we could be sure that the Ce/Sb-SnO_2 catalyst did not detach after using several times. Therefore, we speculated that Ce/Sb-SnO_2 was possessed of hybrid structure and successfully anchored on a ceramic. Because of Ce doping, calcining performance of the prepared samples was improved in the preparation. This also enhanced the densification and conductivity of the prepared samples.

In addition, no impurity peaks are shown in Fig. 5, which shows that the experiments had a good stability. Fig. 5 shows the curves of CV for the Sb-SnO_2 and the Ce/Sb-SnO_2 samples. Theoretically speaking, the areas encircled by CV curve for electrode may demonstrate the conductivity of electrode. This can also indicate that the electrode is possessed of an ability to conduct electric current. By calculating with MATLAB, the areas of the CV curves for the Sb-SnO_2 and the Ce/Sb-SnO_2 membranes are 0.0765 and 0.0899, respectively. Because of Ce doping, Ce/Sb-SnO_2 enjoyed a better conductivity in comparison with Sb-SnO_2 ones.

3.3. Separation of dye from wastewater

3.3.1. Voltage effects

With CF velocities of zero and transmembrane pressure of 0.6 MPa, the membranes with Ce/Sb-SnO_2 were employed to separate dye from wastewater (20 mg L^{-1} dye). In Fig. 6(a), the flux increased with the increase in voltage. High voltage

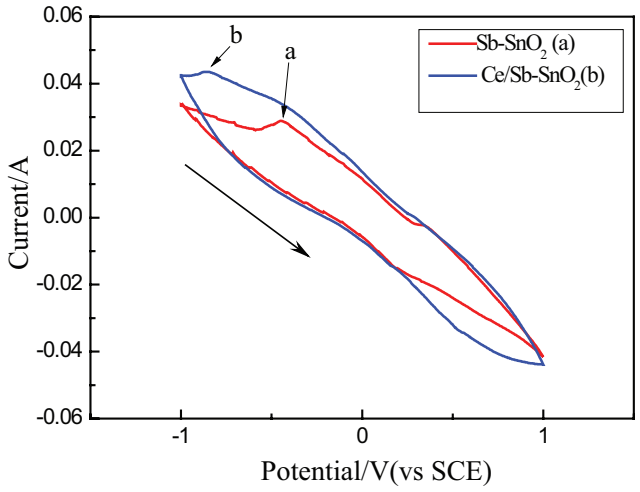

Fig. 5. CV curves of Sb-SnO_2 and Ce/Sb-SnO_2. The arrow represents the scanning direction.

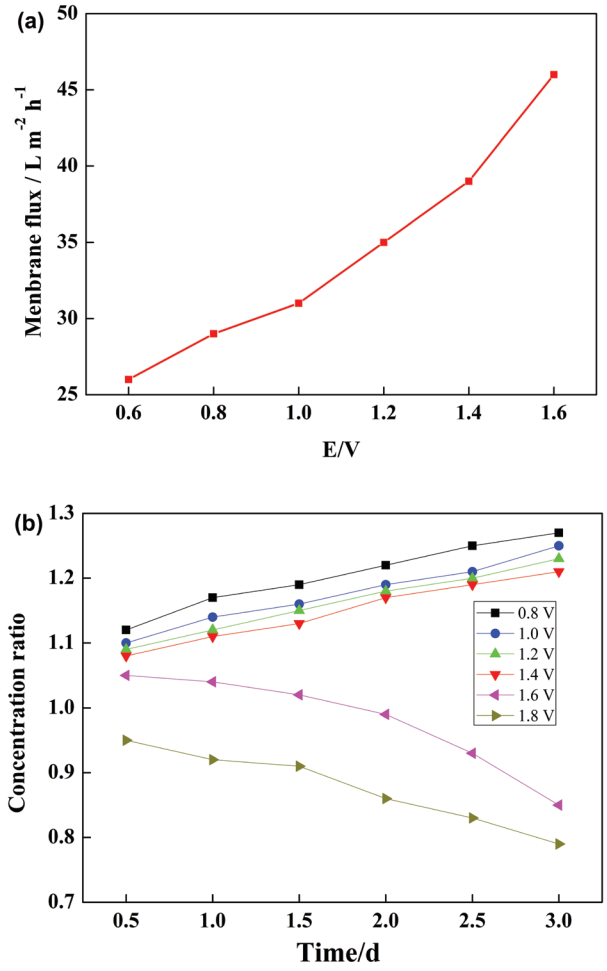

Fig. 6. Effects of voltage on (a) flux and (b) concentration ratio.

contributes to enhancement of the activity of electrocatalyst. This could effectively remove pollutants on the membrane surfaces and reduce membrane fouling on the membrane surfaces, which contributed to the increase in permeation flux. In Fig. 6(b), the concentration ratio (CR) of the dye solution decreased at voltage of over 1.4 V. This indicated that Ce/Sb-SnO_2 had a stronger catalytic activity and produced high concentration of active materials [20,21]. It not only removed pollutants on the membrane surface, but also degraded dye in feed liquid. This resulted in the decrease in dye concentration in feed liquid. A calculation of CR for dye solution is as follows:

$$\mathrm{CR} = \frac{M_{t_2}}{M_{t_1}} \tag{2}$$

Herein, M_{t_1} and M_{t_2} are the values of dye concentration at times t_1 and t_2 (d), respectively. With the voltage of below 1.4 V, Fig. 6(b) shows that dye solution could be concentrated, but the Ce/Sb-SnO_2 membranes had a lower membrane flux in Fig. 6(a). This showed that pollutants plugged some of membrane pores and electrocatalytic oxidation by Ce/Sb-SnO_2 was not strong enough to reduce membrane fouling. The effects of permeation flux could show the degree of membrane fouling. Since electrocatalytic oxidation by the Ce/Sb-SnO_2 could remove pollutants on membrane surface to reduce membrane fouling and give rise to the increase in the flux, the electrocatalytic properties of the Ce/Sb-SnO_2 and the reduction of membrane fouling could be verified by the increase in flux. The results demonstrate that membrane fouling on the surfaces could not be effectively inhibited by Ce/Sb-SnO_2 in the presence of voltage of below 1.4 V.

Based on separation and recycling of dye from wastewater, the authors hoped that the dye in feed liquid was not degraded, and the membrane fouling could be inhibited effectively. All things considered, the voltage 1.4 V was adopted in this study and the Ce/Sb-SnO_2 was possessed of excellent electrocatalytic properties to reduce membrane fouling. In this work, we mainly focused on the effects of electrocatalysis on membrane flux and dye retention. Mechanism of electrocatalytic oxidation to remove pollutants will be investigated in future studies.

3.3.2. *Concentration effects*

In Fig. 7(a), with CF velocity of zero, transmembrane pressure of 0.6 MPa and voltage 1.4 V, the permeation flux decreased with the increase in dye concentration within the range of 10–60 mg L^{-1}. The decrease in the flux was due to the increase in dye concentration which increased the number of dye molecules adsorbed and many membrane pores were plugged. Fig. 7(b) shows that CR declined at dye concentration of 10 mg L^{-1}, which indicated that the dye solution was not concentrated effectively. Since the Ce/Sb-SnO_2 was possessed of an excellent electrocatalytic activity in the presence of voltage 1.4 V, it removed pollutants which plugged membrane pores, and also degraded dye in feed liquid to dilute the solution. In Fig. 7(b), the CR was well obtained at concentration of above 20 mg L^{-1}, but the flux was too low at dye concentration of 60 mg L^{-1} (Fig. 7(a)), which indicated that the pores were plugged and membrane fouling was not reduced effectively. For concentrating dye solution and reducing membrane fouling, all things considered, dye concentration of 20 mg L^{-1} was adopted in this study.

3.3.3. Pressure effects

For obtaining the effects of transmembrane pressure on permeation flux, voltage and dye concentration were kept at 1.4 V and 20 mg L^{-1}, respectively, while the CF velocity of zero was chosen in separation, a pressure played a pivotal role in the change in permeation flux. The number of water molecules through membranes increase with the increase in pressure, which gave rise to the increase in the flux. Fig. 8 shows that the membrane flux increased at pressure range of 0.4–0.7 MPa, but the flux plummeted down at pressure of over 0.7 MPa, which indicated that dye molecules rapidly gathered on membranes surfaces to plug pores. With the increase in pressure, the cake layer on the membrane surfaces quickly formed to block the membrane pores, which led to the flux decline and the membrane fouling.

Fig. 8 demonstrates that flux declined at a pressure of over 0.7 MPa. This indicated that the Ce/Sb-SnO_2 in the presence of voltage 1.4 V could not effectively remove pollutants on the membrane surface. As shown in Fig. 8, the errors of membrane flux were minor at pressure of 0.6–0.7 MPa. All things considered, in order to consume less energy, the pressure of 0.6 MPa was adopted to obtain an optimum flux in this study.

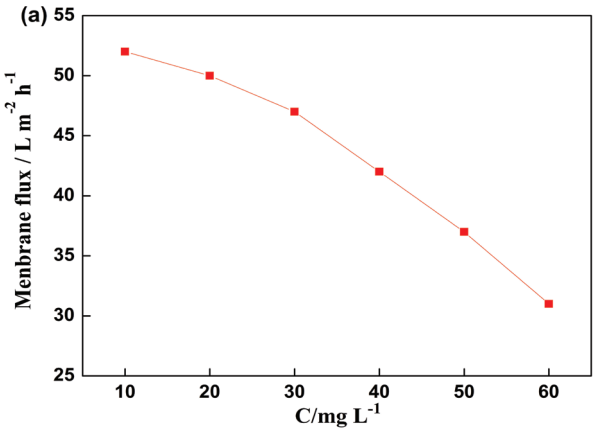

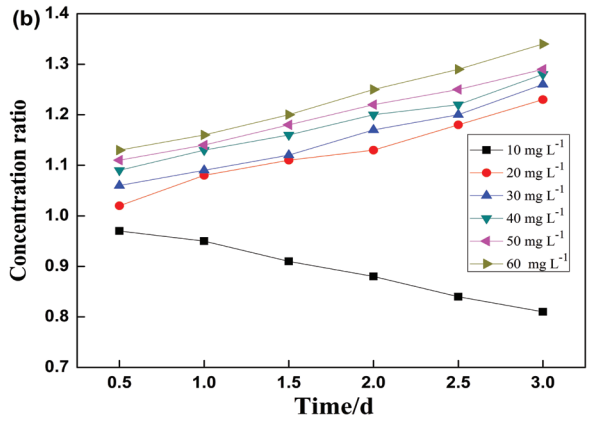

Fig. 7. Effects of dye concentration on (a) flux and (b) concentration ratio.

3.3.4. Retention for dye

With dye concentration of 20 mg L^{-1}, voltage 1.4 V and pressure of 0.6 MPa, retention for dye is shown in Fig. 9. By measuring dye concentration in retentate and permeate solutions, respectively, retention rates for dye can be calculated. In Fig. 9, higher retention rate (99%) for the dye was obtained on Ce/Sb-SnO_2 membrane after 5 d. For Ce/Sb-SnO_2, cerium (Ce) was mixed into Sb-SnO_2 and it affected the crystallinity of Sb-SnO_2 sol and inhibited the growth of Ce/Sb-SnO_2 crystals. Hence, the Ce/Sb-SnO_2 crystals had smaller particulate size and formed nanofiltration membranes with smaller pore diameter in comparison with the Sb-SnO_2 ones. As shown in Fig. 9, the results demonstrated that Ce/Sb-SnO_2 membranes had a higher retention for the dye in comparison with Sb-SnO_2 ones. Hence, we reasonably speculated that Ce/Sb-SnO_2 membranes, compared with the Sb-SnO_2 ones, had a smaller pore size, which was consistent with the computed results (1.95 and 2.86 nm) by molecular weight cut-off of PEG. In future studies, we may also make use of SEM or TEM to prove this fact.

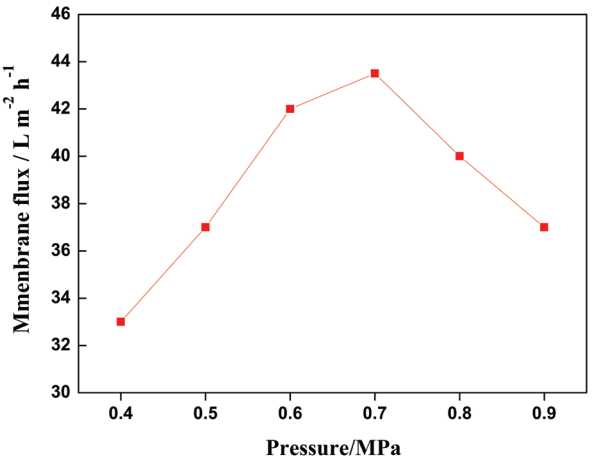

Fig. 8. Effects of pressure on membrane flux at 0.4–0.9 MPa.

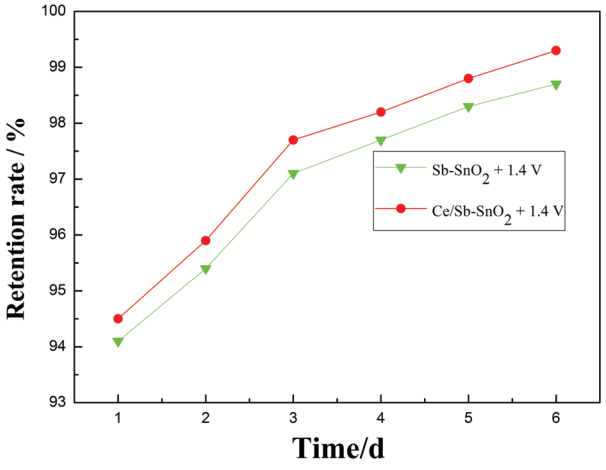

Fig. 9. Effects of Ce/Sb-SnO_2 on retention rate.

In addition, Ce/Sb-SnO_2 sol was loaded on a ceramic to form sample membranes as anode. Therefore, the membrane surface carried positive charge at working. It had an electrostatic repulsion to cationic dye. This also resulted in the increase in retention for the dye.

In this work, the ceramic membranes with the Ce/Sb-SnO_2 were used to separate dyes from wastewater, and the authors mainly focused on the effects of pressure, dye concentration and voltage on the membrane flux and dye retention. Brunauer-Emmett-Teller adsorption of the membranes to dye will be investigated in future studies.

3.3.5. TOC removal

A removal rate for total organic carbon (TOC) is also an important parameter evaluating the effects of membrane separation. For obtaining the removal rates for TOC, pressure, dye concentration and voltage were kept at 0.6 MPa, 20 mg L^{-1} and 1.4 V, respectively. By measuring concentration for TOC in retentate and permeate solutions, a calculation of TOC removal rate can be shown as follows:

$$\text{TOC}\% = \frac{M_1 - M_2}{M_1} \times 100\% \quad (3)$$

Herein, M_1 and M_2 are the TOC value at retentate and permeate solutions, respectively. In Fig. 10, a removal rate of 99% for TOC was obtained on the Ce/Sb-SnO_2 membrane in the absence of power supply after 6 h, which showed that dye concentration was very low in permeate solution. This also indicated that the Ce/Sb-SnO_2 membrane had a good ability to intercept dye in feed liquid. A removal rate for TOC could reach 79% on this membrane in the presence of voltage 1.4 V after 6 h. Since electrocatalytic oxidation-degraded dye adsorbed on the membrane surface (or within pores), degradation products (small molecules) passed through membrane pores to permeate solution. Hence, the TOC concentration increased in penetrating fluid. This resulted in the decrease in TOC removal rates, and also showed that Ce/Sb-SnO_2 was possessed of an ability to remove pollutants on membrane surface and to reduce the membrane fouling.

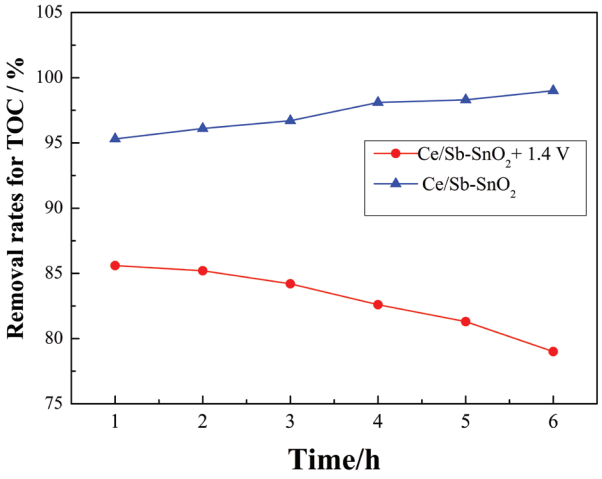

Fig. 10. Effects of Ce/Sb-SnO_2 on removal rate of TOC.

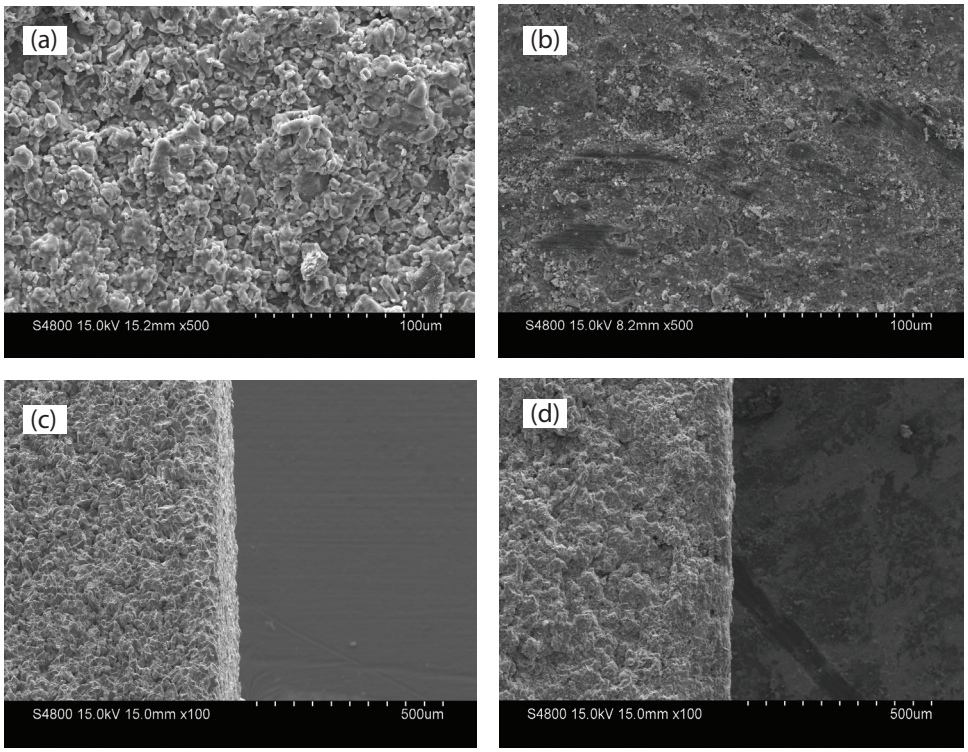

Fig. 11. Surface and section morphology of the working membranes: (a) surface 15.2 mm × 500 SEM; (b) surface 8.2 mm × 500 SEM; (c) section 15.0 mm × 100 SEM and (d) section 15.0 mm × 100 SEM.

Before this working membrane, its morphology is shown in Fig. 2(c) and this membrane surface was clean. After the Ce/Sb-SnO_2 membranes worked for 6 h in the absence of power supply, the morphology of the membrane surface and section is shown in Figs. 11(a) and (c), respectively. In Fig. 11(a), a multitude of pollutants accumulated on the membrane surface to cause membrane fouling serious. After the membrane with Ce/Sb-SnO_2 worked for 6 h in the presence of voltage 1.4 V, its surface and section morphology are shown in Figs. 11(b) and (d), respectively. By comparing Figs. 11(a) with Fig. 11(b), it is seen from Fig. 11(b) that the lots of pollutants on the surface were obviously removed. It seems that the membrane surface in Fig. 11(b) is cleaner than that in Fig. 11(a). However, there are not many differences between Figs. 11(c) and (d). We speculated that the pollutants adsorbed into membrane pores were not drastically removed by electrocatalytic oxidation.

4. Conclusions

Characterization of sample membrane reveals the membrane containing Ce, Sb and SnO_2. A Ce/Sb-SnO_2 was loaded on a ceramic for synthesizing electrocatalytic membranes, and the electrocatalytic reaction and nanofiltration process can carry out at the same time. With the Ce/Sb-SnO_2 membranes in the presence of voltage 1.4 V, dyestuff was separated from wastewater and the membrane fouling was reduced. Ce/Sb-SnO_2 membranes are stable and reusable.

Acknowledgement

The support from the Zhejiang Provincial Technology Application Research Foundation (2011C31031) is highly appreciated.

References

[1] B. Liang, Q. Yao, H. Cheng, S. Gao, F. Kong, D. Cui, Y. Guo, N. Ren, A. Wang, Enhanced degradation of azo dye alizarin yellow R in a combined process of iron-carbon micro-electrolysis and aerobic bio-contact oxidation, Environ. Sci. Pollut. Res., 19 (2012) 1385-1391.

[2] L. Qin, G. Zhang, Q. Meng, L. Xu, B. Lv, Enhanced MBR by internal micro-electrolysis for degration of anthraquinone dye wastewater, Chem. Eng. J., 210 (2012) 575-584.

[3] S. Wang, D. Li, C. Sun, S. Yang, Y. Guan, H. He, Synthesis and characterization of g-C_3N_4/Ag_3VO_4 composites with significantly enhanced visible-light photocatalytic activity for triphenylmethane dye degradation, Appl. Catal., B, 144 (2014) 885–892.

[4] S. Zhao, Z. Cheng, L. Kang, Y. Zhang, X. Zhao, A novel preparation of porous spong-shaped Ag/ZnO heterostructures and their potent photocatalytic degradation efficiency, Mater. Lett., 182 (2016) 305–308.

[5] S.V. Babu, S. Raghupathy, M. Rajasimman, Optimization of anaerobic conditions for the treatment of textile dye wastewater using mixed culture, J. Environ. Sci. Pollut. Res., 2 (2016) 50-53.

[6] F. Carlesso, G. Zin, S.M. de Souza, M.D. Luccio, A.A. de Souza, J.V. Oliveira, Magnetic field on fouling control of ultrafiltration membranes applied in treatment of a synthetic textile effluent, Environ. Technol., 37 (2016) 952-959.

[7] B. Sarkar, S. De, Prediction of permeate flux for turbulent flow in cross flow electric field assisted ultrafiltration, J. Membr. Sci., 369 (2011) 77-87.

[8] E. Brillas, C.A. Martínez-Huitleb, Decontamination of wastewaters containing synthetic organic dyes by electrochemical methods. An updated review, Appl. Catal., B, 166–167 (2015) 603–643.

[9] B. Xiong, Y. Zhou, Y. Zhao, J. Wang, X. Chen, R. O'Hayre, Z. Shao, The use of nitrogen-doped graphene supporting Pt nanoparticles as a catalyst for methanol eletrocatalytic oxidation, Carbon, 52 (2013) 181-192.

[10] M. Sun, F. Zhang, Z.H. Tong, G.P. Sheng, Y.Z. Chen, Y. Zhao, Y.P. Chen, S.Y. Zhou, G. Liu, Y.C. Tian, H.Q. Yu, A gold-sputtered carbon paper as an anode for improved electricity generation from a microbial fuel cell inoculated with *Shewanella oneidensis* MR-1, Biosens. Bioelectron., 26 (2010) 338-343.

[11] N. Wang, T. Jiang, Y. Yang, C. Wu, L. Guan, Facile coating carbon nanotubes with metal oxide nanoparticles of controlled size, Chem. Phys. Lett., 605–606 (2014) 35-37.

[12] H. Dong, K. Xiao, W. Liu, S. Guo, Enhancement of ultrafiltration with a γ-Al_2O_3 ceramic membrane by an electrical field, Desal. Wat. Treat., 49 (2012) 234–239.

[13] H. Dong, K. Xiao, X. Li, Y. Ren, S. Guo, Preparation of PVDF/Al_2O_3 hybrid membrane via the sol-gel process and characterization of the hybrid membrane, Desal. Wat. Treat., 51 (2013) 3685–3690.

[14] H. Dong, K. Xiao, X. Tang, Z. Zhang, J. Dai, R. Long, W. Liao, Preparation and characterization of polyurethane (PU)/polyvinylidene fluoride (PVDF) blending membrane, Desal. Wat. Treat., 57 (2016) 3405–3413.

[15] A.N. Subba Rao, V.T. Venkatarangaiah, Metal oxide-coated anodes in wastewater treatment, Environ. Sci. Pollut. Res., 21 (2014) 3197-3217.

[16] F.L. Zhu, Y.S. Meng, X.Y. Huang, Electro-catalytic degradation properties of Ti/SnO_2–Sb electrodes doped with different rare earths, Rare Met., 35 (2016) 412-418.

[17] Y. Duan, Q. Wen, Y. Chen, T. Duan, Y. Zhou, Preparation and characterization of TiN-doped Ti/SnO_2-Sb electrode by dip coating for Orange II decolorization, Appl. Surf. Sci., 320 (2014) 746-755.

[18] C. Cheng, Z.J. Jiang, C.Y. Liu, Plus green emission of ZnO nanorods induced by Ce^{3+} doping and concentration, J. Photochem. Photobiol., A, 195 (2008) 151-155.

[19] P. Puhlfürß, A. Voigt, R. Weber, M. Morbé, Microporous TiO_2 membranes with a cut off <500 Da, J. Membr. Sci., 174 (2000) 123-133.

[20] A. Cano, P. Cañizares, C. Barrera-Díaz, C. Sáez, M.A. Rodrigo, Use of conductive-diamond electrochemical-oxidation for the disinfection of several actual treated wastewaters, Chem. Eng. J., 211–212 (2012) 463-469.

[21] L. Li, Y. Liu, Ammonia removal in electrochemical oxidation: mechanism and pseudo-kinetics, J. Hazard. Mater., 161 (2009) 1010-1016.